Journal of Colloid and Interface Science **252,** 383–392 (2002)
doi:10.1006/jcis.2002.8494

Multilevel Structure of Sludge Flocs

R. M. Wu,* D. J. Lee,*,[1] T. D. Waite,† and J. Guan†

*Department of Chemical Engineering, National Taiwan University, Taipei, Taiwan 10617; and †School of Civil and Environmental Engineering, University of New South Wales, Sydney, New South Wales 2052, Australia

Received August 20, 2001; accepted May 20, 2002

In this work, the structure of two kaolin sludges and a waste activated sludge are investigated using both light-scattering and free-settling methods. Fractal dimensions estimated by the light-scattering and free-settling techniques (D_S and D_F respectively) differ significantly and support the hypothesis that naturally occurring aggregates possess a multilevel structure. A two-level floc structural model comprised of (i) a primary floc (of fractal dimension D_S) consisting of primary particles and (ii) a secondary floc (of fractal dimension D_F) consisting of the microflocs is proposed to interpret the experimental findings. The structural changes of sludge flocs before and after cationic flocculation are interpreted using the proposed two-level model. © 2002 Elsevier Science (USA)

Key Words: **floc structure; light scattering; free settling; fractal dimension.**

INTRODUCTION

Some researchers have proposed that a sludge floc be considered to be a highly porous fractal-like aggregate of many primary particles (1, 2). Li and Ganczarczyk (3) sliced activated sludge flocs to examine cross-sectional morphology, confirming their fractal-like interior structure. Zartarian *et al.* (4) demonstrated the fractal morphology in an activated sludge floc using three-dimensional reconstruction. An important parameter that characterizes a fractal object is the fractal dimension, $D(-)$, which corresponds to the space-filling capacity of an object. The mass M of a fractal object with fractal dimension D can be considered to be proportional to its diameter d_f:

$$M \propto d_f^D, \qquad [1]$$

where $1 \leq D \leq 3$. The aggregates generated in water and wastewater treatment processes exhibit fractal dimensions ranging from 1.4 to 2.8 (1).

Free-settling tests are widely employed in estimating the fractal dimension of sludge flocs (1, 3, 5–10). Lee *et al.* (11) critically reviewed the use and constraints of the free-settling test. The fractal dimension of flocs can also be determined using light-scattering methods. Many investigators, including Axford and Herrington (12), Zhang and Buffle (13), Kyriakidis *et al.* (14), Jung *et al.* (15), and Guan *et al.* (16, 17), have used small-angle light scattering to study the structure of flocs. Guan (18) briefly summarized the limits of the light-scattering test. Different measuring techniques should lead to a similar estimate of the fractal dimension of the flocs in a sludge if the floc structure could be characterized by a single fractal dimension.

When an aggregate is formed by the action of a unique mechanism (e.g., diffusion-limited aggregation), a single fractal dimension is sufficient to characterize the interior structure. However, aggregates occurring naturally may have multilevel structure (19–21). Gorczyca and Ganczarczyk (22) proposed an activated sludge model that includes the following stages: (1) primary particles form flocculi, (2) flocculi group together to form microflocs, and (3) microflocs form the flocs. Flocculi, microflocs, and flocs can exhibit different structures and perhaps different fractal dimensions. An activated sludge floc can therefore be viewed as a multifractal object (23). Two or more fractal dimensions may thus be required to characterize a sludge floc. Employing different estimating methods on a specific aggregate that exhibits multilevel structure could lead to different estimates of fractal dimension (as shown later) if these techniques probe structure at different length scales.

This issue is investigated here using small-angle light-scattering and free-settling methods to examine the structure of both activated sludge flocs and assemblages of kaolinite particles before and after addition of a polymeric flocculant. A two-level model is proposed to interpret the structural changes of flocs after polyelectrolyte-induced flocculation. In the following section, we briefly summarize the basic principles of the two measurement methods used.

ESTIMATION OF FRACTAL DIMENSION

Light-Scattering Test

The light-scattering technique involves measurement of light intensity I as a function of the wave vector, Q. This vector is defined as the difference between the incident and scattered wave vectors of the radiation beam in the medium. The magnitude of the wave vector can be approximated as follows:

$$|\vec{Q}| = Q = \frac{4\pi n \sin(\theta/2)}{\lambda}, \qquad [2]$$

[1] To whom correspondence should be addressed. Fax: +886-2-2362-3040. E-mail: djlee@ccms.ntu.edu.tw.

0021-9797/02 $35.00

where n, θ, and λ are the refractive index of the medium (−), the scattered angle (−), and the wavelength of radiation in vacuum (m), respectively. In scattering theory, the scattering intensity $I(Q) \propto F(Q)S(Q)$, where $F(Q)$ and $S(Q)$ are the form factor and the structure factor, respectively. The form factor is related to the shape of the particle, while the structure factor accounts for the interparticle correlations describing the spatial arrangement of the particles.

A plot of log I versus log Q is shown in Fig. 1a. In the regime $QR_p \gg 1$, where R_p is the primary particle size,

$$I(Q) \propto Q^{-4}, \quad [3]$$

which is Porod's law and reflects scattering from the primary particle surfaces. In the region where $QR \ll 1$ (Guinier regime), the form factor $F(Q)$ is roughly constant. If the inequality

$$1/R \ll Q \ll 1/R_p \quad [4]$$

holds and individual particles scatter light independently such that the total scattered wave is the sum of the scattered waves from each particle (the Rayleigh–Gans–Debye [RGD] approximation), then one obtains

$$I(Q) \propto Q^{-D}. \quad [5]$$

This region is recognized as the fractal regime, where the mass fractal dimension (D) reflects the internal structure of the fractal clusters (24). The mass fractal dimension describes the space-filling ability of the aggregate and, as mentioned earlier, can vary from 1 (a linear aggregate) to 3 (a compact or space-filling form). As the length scale corresponding to the Q value approaches the aggregate size ($Q \cong 1/R$), the Q^{-D} relationship starts to be influenced by the edge of the aggregate and hence the structure cannot be determined in such regions (24). The fractal dimension, D, can thus be estimated from the slope of $I(Q)$ versus Q data by fitting a straight line through the section of the scattering plot in the fractal regime. High size polydispersity, as might be expected for activated sludge flocs, would be expected to limit the length scale over which fractal behavior is observed because polydispersity may lead to deviation from linearity at larger length scales (smaller Q) (25).

As noted above, the simple power law relationship between I and Q in the fractal regime is valid provided the particles scatter light independently. In reality, there are always secondary and higher order waves that are scattered more than once. Hence, certain conditions need to be fulfilled for the RGD approximation to be satisfied (26). They are

$$|m - 1| \ll 1 \quad [6]$$

$$(2\pi n/\lambda)L|m - 1| \ll 1, \quad [7]$$

where m is the relative refractive index of the scatterers and L is the length of the scattering body. As noted by Selomulya *et al.* (27), a study by Farias *et al.* (28) comparing the absorption, total, and angular scattering cross sections predicted by RGD and by an integral formulation of the scattering intensity showed that the range of validity of the RGD theory can be extended beyond the range specified above. Deviation of less than 10% can be achieved for conditions where $|m - 1| \leq 1$ and $\frac{2\pi n}{\lambda} L\,|m - 1| \leq 0.6$. For aggregates constructed from primary particles with low refractive index (e.g., the bacterial aggregates being investigated here), the RGD assumption can be applied for much larger assemblages than indicated by Eq. [7]. Furthermore, the measure of D (assuming the RGD approximation is valid) is acquired from the slope of the logarithmic $I(Q)$ versus Q instead of the absolute scattering

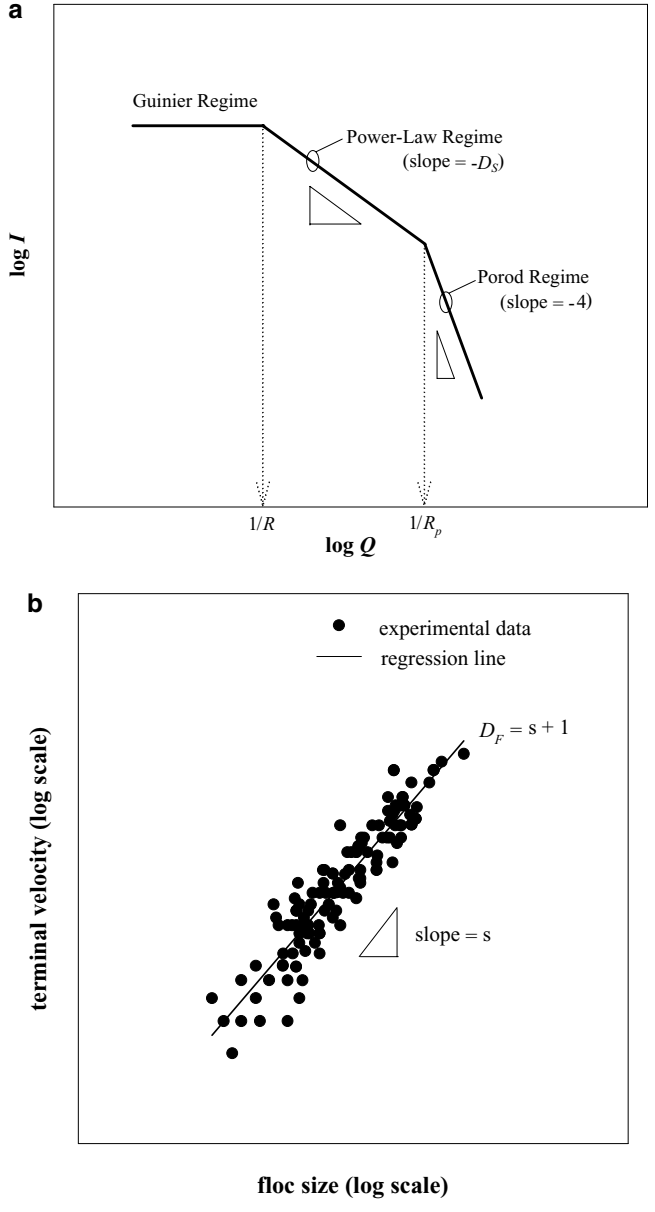

FIG. 1. Determination of fractal dimension of sludge flocs. (a) Small angle light-scattering test. (b) Free-settling test.

intensity values, and thus even this limit may still be too conservative (29).

In summary, then, the log–log plot of I versus Q from data collected in scattering tests should exhibit a linear character with a slope of $-D$ in the fractal scattering region. The fractal dimension estimated according to the light-scattering test is herein referred to as D_S. Moreover, the transition points in Fig. 1a provide preliminary estimates of R and R_p.

Free-Settling Test

Consider a floc moving steadily through a quiescent, infinitely large fluid pool. The drag force exerted on the floc can be expressed as

$$F_D = (\pi R^2)\left(\frac{1}{2}\rho V^2\right) C_D \Omega, \quad [8]$$

where C_D = drag coefficient (−), V = floc moving velocity (m/s), ρ = fluid density (kg/m^3), and Ω = ratio of the resistance experienced by a floc to that experienced by an equivalent solid sphere (−). Lee *et al.* (11) discussed the information required to evaluate Eq. [8]. For a highly porous sphere, the drag force can be rearranged as follows (30):

$$F_D = \frac{A(\beta)}{8}\pi\mu V d_f, \quad [9]$$

where μ = liquid viscosity (Pa-s), d_f = diameter of floc (m), and $A(\beta)$ = correction factor accounting for the advection flow through the floc interior over a wide range of Reynolds numbers (−). Hence, for a floc moving steadily in an infinite medium, the balance between buoyant weight and the hydrodynamic drag force is represented by the following equality:

$$\rho_f - \rho = \frac{3A(\beta)}{4}\frac{\mu V}{g d_f^2}. \quad [10]$$

The density versus floc velocity relation for a fractal aggregate whose mass–size relationship follows Eq. [8] can be expressed as follows:

$$\rho_f - \rho = C d_f^{D-3}, \quad [11]$$

where C is a proportionality constant (kg-m^{-D}). Restated, the density of a fractal aggregate decreases with increasing floc size. Inserting Eq. [11] into Eq. [10] leads to the following equality:

$$V = \frac{4C}{3A(\beta)}\frac{g}{\mu} d_f^{D-1}. \quad [12]$$

If the correction factor $A(\beta)$ can be regarded as a constant over the range of Reynolds numbers investigated (an approximation that is often found to be valid), then the log–log plot of the floc terminal velocity versus the floc size is a line of slope $D - 1$ (31). Figure 1b schematically depicts the free-settling test data. The fractal dimension estimated by the free-settling test is referred to as D_F in this study.

EXPERIMENTAL

The Samples

The internal structures of aggregates derived from kaolin slurries and an activated sludge are investigated in this article.

The particle size distribution of the kaolin slurry was determined using a Micromeritics 5100C sedigraph and found to be a relatively monodispersed distribution with a mean diameter of approximately 2.3 μm. The true solid density was determined using a Micromeritics Accupyc 1330 pycnometer and found to be 2727 kg/m^3 with a relative deviation of less than 0.5%. The kaolin slurry was prepared by mixing 17 or 8% w/w kaolin powder and 10^{-1} M $NaClO_4$ in distilled water. $NaClO_4$ was added to provide a high enough ionic strength to prevent interference of other ions that might be released from the kaolin particle surfaces. The pH was adjusted to around 7.0 using $HClO_4$ and NaOH. Flocculated kaolin sludge was prepared by mixing the weighted suspension with cationic polymer T-3051 from Kai-Guan (Taiwan). The polymer T-3051 is a polyacrylamide with an average molecular weight of 10^7 and a charge density of 20%. The polymer solution was gradually poured into a mixing vessel at a stirring speed of 200 rpm for about 5 min and then at 50 rpm for 20 min.

The activated sludge samples were taken from St. Mary's sewage treatment plant in Sydney, Australia, which handles 37,000 m^3/day wastewater using primary, secondary, and tertiary treatment processes. The raw sewage is screened, degritted, and clarified in the primary clarifiers. The primary treated sewage then undergoes conventional activated sludge treatment, where part of the waste activated sludge from the secondary clarifiers is recycled back to the aeration tanks. It was from this recycle stream that the activated sludge sample (of pH 6.43) was taken. The polymer Zetag 92, supplied by Ciba, was used to condition the sludge samples. The sludge sample and flocculant were mixed at 400 rpm for 30 s and then at 150 rpm for 1 min. The polymer was of 10^6 to 10^7 molecular weight and is made up of random copolymers of acrylamide and dimethyl amino ethyl acrylate.

A zeta meter (Zeter-Meter System 3.0, Zeter-Meter) was used to measure zeta potentials of the particles of interest. The zeta potentials for the 8 and 17% kaolin slurries were −17.8 and −25.3 mV, respectively. The activated sludge sample exhibited a zeta potential of −35.2 mV.

A capillary suction apparatus was used to estimate the sludge filterability. The inner cylinder radius was 0.535 cm. The time required for the filtrate to migrate from 1.5 to 2.5 cm was defined as the capillary suction time (CST). Whatman No. 17 paper was used as the filter paper.

The chemical oxygen demand (COD) and suspended solids (SS) content of the supernatant of waste activated sludge that had settled for 10 min were determined to be 41 and 90 mg/L,

respectively. The percentage by weight of dry mass in the original activated sludge was estimated by weighing and drying and found to be 0.55% w/w. The particle size distribution (PSD) was determined using a Coulter LS230 particle size analyzer. The mean floc size for the original activated sludge was 138 μm.

Light-Scattering Test

Small-angle laser light scattering tests were conducted using a Malvern Mastersizer/E, which consists of a 5-mW He-Ne laser ($\lambda = 632.8$ nm) as the light source and an optic lens and photosensitive detectors. The scattered light was collected at angles between 0.03 and 6.52° using a 31-element solid state detector array. The light obscuration level of samples had to be maintained between 10 and 30% for reliable measurements; thus, samples were diluted to appropriate levels prior to analysis. As shown previously by Guan *et al.* (17), analysis at excessive obscurations leads to significant underestimation of scattering exponents. The Malvern Mastersizer/E was also used to measure the aggregate size between 1.2 and 600 μm. Approximately 20 measurements of floc size and structure were taken over a period of 400 s to assess the consistency (and any time dependency) of results. A small magnetic stirrer was installed in the scattering chamber to suspend the sample particles. The induced current did not markedly affect the scattered intensity from samples. Such a stirrer is essential for reliable measurement, especially for flocculated sludge particles whose sizes, which determine the sedimentation velocities, are generally large.

Free Settling Test

Two transparent containers, one rectangular of 2×2 (width $\times$ length) $\times$ 15 cm (height) and the other cylindrical of 6 cm in diameter and 50 cm in height, were used for the floc-settling studies. The largest floc size considered was around 400 to 500 μm, giving an aspect ratio (floc size/container size) of greater than 100. Wu and Lee's results (31) demonstrated that side wall effects could be safely neglected. A JVC camera equipped with a close-up lens was used to record the floc motion. A floc was released carefully from the top of the column. The floc diameters normal to and parallel to the vertical direction were measured. The center of mass of the floc was calculated using the images recorded during each interval. The terminal velocity of the floc could be subsequently estimated from the floc position versus time data.

RESULTS

Sludge Dewaterability and Floc Size

Figures 2a and 2b display the measured zeta potentials and CST data for the kaolin slurries and the activated sludge. The surface charge of the suspended particles in kaolin sludges was neutralized at polymer concentrations of 260 ppm for 8% and 600 ppm for 17% w/w suspensions. These dosages are highlighted in Fig. 2a using broad arrows. For kaolin slurries, their CST–polymer dose curves reach a minimum close to the charge neutralization points. These doses are referred to as "optimum doses" in this work and are shown as thin arrows. Hence, charge neutralization would appear to be essential for determining the polyelectrolyte flocculation efficiency for the kaolin slurry.

The surface charge of the particles in waste activated sludge reduces to zero at a polymer dose of approximately 45 ppm (Fig. 2b). The minimum CST occurs at a dose ranging from 10 to 30 ppm. In comparison with the kaolinite case, the flocculation of the activated sludge sample could be governed by a bridging mechanism rather than charge neutralization.

Figure 3a demonstrates the floc size for the original and the flocculated kaolin sludges. The floc size for the original slurry is approximately 28 μm at the start of testing, indicating that the high ionic concentration in the suspension (0.1 M $NaClO_4$) has resulted in particle coagulation ($R_p = 2.3\mu$m). During the 400 s following coagulation, the floc size increases slightly to 40 μm, possibly due to flocculation effects induced by the magnetic stirrer in the scattering chamber. The application of polyelectrolyte flocculation markedly increases the floc size to 200 to 350 μm, depending on the sludge species and the polymer dose. A higher polymer dose leads to larger floc size, suggesting a favorable flocculation. Applying an optimal dose of polyelectrolyte did not alter the trend in floc growth. Moreover, the floc size of flocculated 8% suspension is larger than that in the 17% suspension (Fig. 3b).

The change in floc size for activated sludge resembles that for kaolin sludges. As Fig. 3c shows, the floc size for the original activated sludge remains at around 135 to 140 μm independent of the scattering time. Applying polymer doses of 10, 30, and 60 ppm increases the floc size to 170, 280, and 360 μm, respectively. No correlation between the occurrence of the optimal dose (i.e., that yielding minimum CST) and the floc size growth is apparent.

Light Scattering Tests

Figure 4 demonstrates the log–log plot of I against Q for the original kaolin sludges and for the activated sludge. On each log I versus log Q curve, two linear regimes divided at $Q = Q_C$ (the arrows) are evident. As discussed earlier, $Q < Q_C$ represents the Guinier regime, while $Q > Q_C$ is the power law regime. The transition point Q_C corresponds to $1/R$. We observe no regime at high Q following Porod's law. The two curves for the 8 and 17% kaolin sludges are close to each other, with their corresponding Q_C values similar. Interestingly, the Q_C values for the kaolin sludges prior to polymer addition are in the vicinity of 1.5×10^{-4} nm^{-1}, yielding an upper scattering size of around 6.5 μm. This is significantly less than the mean size of 28 μm determined by light scattering and only marginally greater than the mean size of primary particles. This result suggests that aggregates of only a few primary particles exhibit fractal structure, with structures at larger length scales apparently lacking the coherence to generate power law light-scattering behavior.

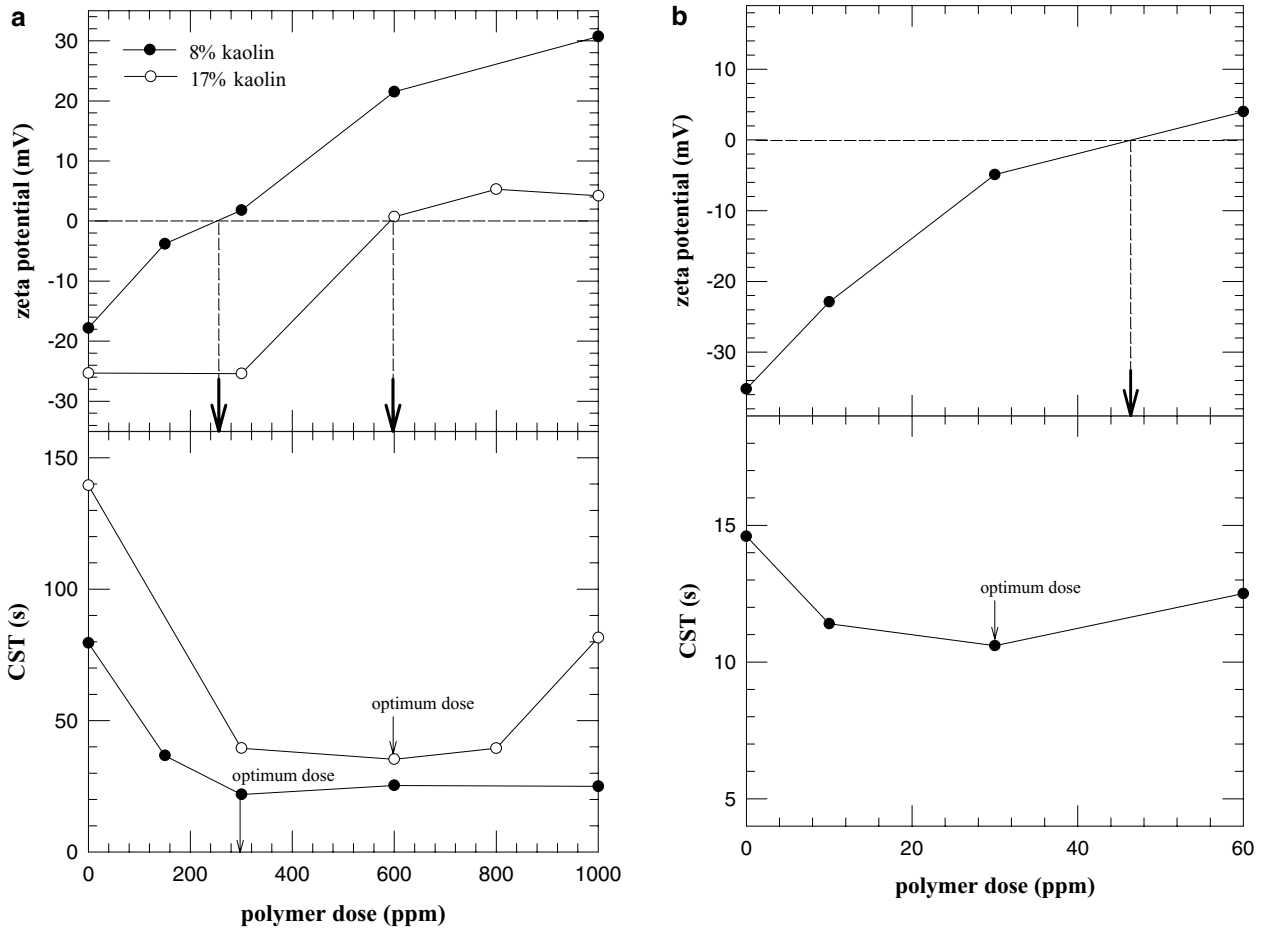

FIG. 2. The zeta potentials and capillary suction time (CST) data versus polyelectrolyte dose. (a) Kaolin sludge. (b) Activated sludge.

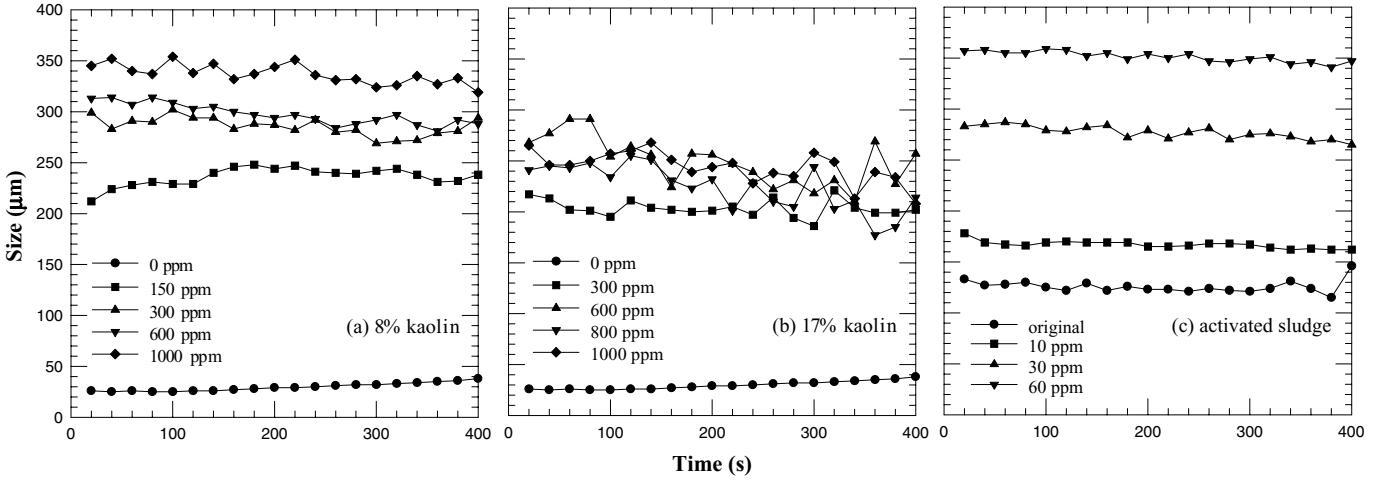

FIG. 3. The floc size of original and flocculated sludge. (a) 8% kaolin sludge. (b) 17% kaolin sludge. (c) Activated sludge.

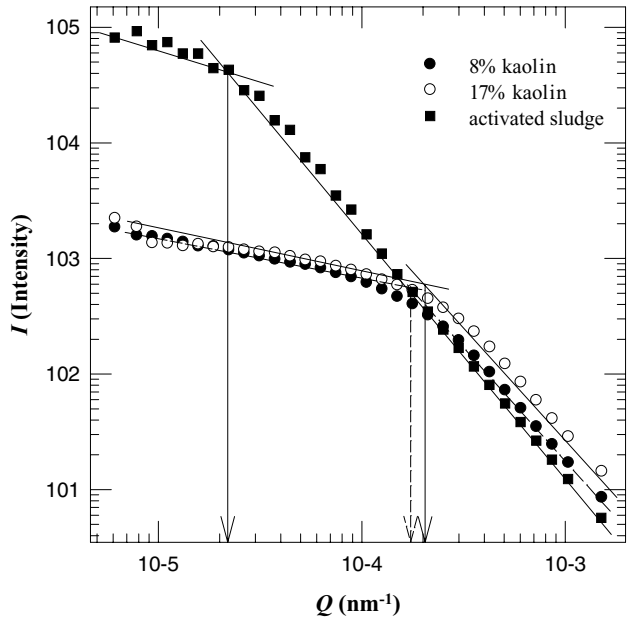

FIG. 4. The log–log plot of I as a function of Q for the original kaolin sludges and for the activated sludge. Arrows denote the position where $Q = Q_C$.

The curve for activated sludge exhibits a much wider power law regime than do the kaolin sludge cases with a Q_C value of approximately 2×10^{-5} nm^{-1} corresponding to an upper fractal scattering size of around 50 μm. This scattering size is still significantly less than the measured mean size of activated sludge flocs of approximately 140 μm either as a consequence of highly variable compactness at larger length scales or (more likely) as a result of heterogeneity in aggregate size and associated edge effects.

According to Fig. 1a, the fractal dimension of the suspension can be estimated by linearly regressing the data in the power law regime. To ensure that we are well clear of any size polydispersity effects, we have restricted analysis to the 10^{-3} to 10^{-4} nm^{-1} Q range. The slopes of the curves for the two kaolin sludges are close, giving similar fractal dimensions (1.97–1.99). The slope of the log I versus log Q data for the activated sludge sample in the power law region is -2.12, suggesting a slightly more compact floc than is observed for the kaolinite flocs. This value for the activated sludge floc is similar to that reported by Guan *et al.* (17). Note that while multiple scattering effects are expected to be insignificant for assemblages of $D_S < 2$, multiple scattering may occur for the more compact flocs (32, 33). In this event, the light scattered at any Q value may be less than otherwise expected. Multiple scattering will be operative across the Q range, however, and at least over the narrow Q range used for D_S determination, the effect on the slope of the log I versus log Q plots is expected to be minimal (28).

The scattering data for the sludges flocculated by polymer addition are shown in Fig. 5. The original sludges are also included in this figure for comparison. Distinct changes are apparent in the scattering data for kaolin. Most distinctively, the Guinier region for both the 8 and 17% kaolin sludges occurs at a much lower Q value than in the polymer-free case. Q_C values in the 1 to 2×10^{-5} nm^{-1} region (corresponding to R values of 50–100 μm) are observed in the presence of polymer as compared with the polymer-free case of around 1.5×10^{-4} nm^{-1} ($R = 6.5$ μm). While the scattering data is reasonably linear over this expanded Q range, slight upward curvature at low Q is apparent in some instances. This apparent increase in compactness at larger length scales may result from restructuring effects arising from the slow stirring that is used to maintain the flocs in suspension. In light of this, D_S values have been estimated over a similar Q range to that used in the nonpolymer case.

In the activated sludge case, polymer addition also leads to an increase in the size range over which fractal scattering occurs, but the upper limit is difficult to ascertain because it exceeds the examinable Q range. Upward curvature is again apparent at low Q, particularly for the larger flocs. As a result, we have again

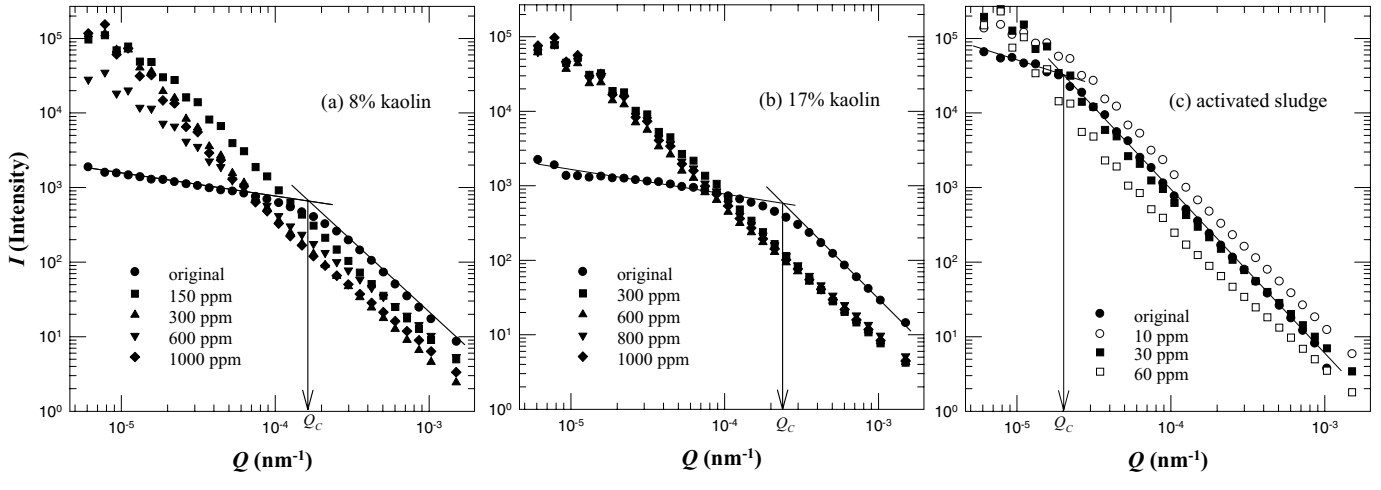

FIG. 5. The log–log plot of I as a function of Q for the original and flocculated sludge. (a) Kaolin sludge, 8% w/w. (b) Kaolin sludge, 17% w/w. (c) Activated sludge.

TABLE 1
Estimated Fractal Dimensions of Kaolin and Activated Sludges

8% kaolin	Original	150 ppm	300 ppm$^+$	600 ppm	1000 ppm
D_S	1.98 ± 0.01	1.85 ± 0.06	1.83 ± 0.02	1.64 ± 0.01	1.68 ± 0.01
D_F	NA	2.31	1.86	2.16	1.98
17% kaolin	Original	300 ppm	600 ppm$^+$	800 ppm	1000 ppm
D_S	1.98 ± 0.02	1.76 ± 0.07	1.72 ± 0.01	1.73 ± 0.01	1.77 ± 0.01
D_F	NA	2.12	1.9	1.98	1.94
Activated sludge	Original	10 ppm$^+$	30 ppm	40 ppm	—
D_S	2.12 ± 0.02	2.06 ± 0.02	1.94 ± 0.01	1.85 ± 0.03	—
D_F	1.55	1.31	1.34	1.48	—

Note. D_S: based on small angle light-scattering tests; D_F: based on free-settling tests. The superscript "+" indicates the optimum dosing regime. NA: not available.

restricted slope measurement for the purposes of D_S procurement to the 10^{-3} to 10^{-4} nm^{-1} Q range (the same as that used in the polymer-free case).

Table 1 summarizes the estimated D_S results. The addition of polyelectrolyte up to 1000 ppm reduces the fractal dimension of kaolin sludges from around 2.0 to 1.6 to 1.7. The corresponding fractal dimension for activated sludge falls monotonically from 2.14 to 1.85 for increasing polymer doses (up to 40 ppm). Restated, the presence of the polymer leads to a more open floc structure than is evident in the undosed sludge. Such a finding, together with the much larger floc size (Fig. 3), demonstrates that polymer flocculation could generate large flocs with highly permeable interior that are more readily dewatered.

When the sludge is overdosed, the floc size tends to increase continuously, but the D_S value rises slightly again. The CST values in Fig. 2 suggest a deteriorating dewaterability in the overdosing regime. Here, the packing characteristics of the primary particles within a floc aggregate appear to play a more essential role than does the floc size in determining the sludge dewaterability.

Free-Settling Test

The results of the free-settling tests are summarized in Fig. 6. Note that the aggregates in the original (nonflocculated) kaolin sludges are generally too small for reliable free-settling measurements using the current apparatus. For such sludges, the free-settling tests are therefore neglected. In the other tests, at the same floc size, the settling velocity of the kaolin floc is much higher than of the activated sludge floc. Moreover, the flocculated sludge flocs generally exhibit a higher settling velocity than do the original sludge flocs.

A log–log plot of settling velocity versus floc size exhibits a linear correlation, indicating the feasibility of using Eq. [10] for interpreting data. Because we have no detailed information regarding the correction factor $A(\beta)$ and the proportionality constant C in Eq. [10] for the current sludge samples, only the fractal dimension of aggregates could be obtained using linear regression analysis. Table 1 summarizes the measured D_F values.

Three particular observations arise from Table 1. First, the D_F value for the original activated sludge is estimated to be 1.55, which correlates with literature results (10). Second, the estimated D_F value decreases initially with added polymer. After reaching a minimum value at the optimum dose, the D_F value increases again. For instance, the estimated D_F value decreases from 1.55 for the original activated sludge down to 1.31 to 1.34 at a polymer dose of 10 to 30 ppm. At 60 ppm, the fractal dimension rises again to 1.48. That is, the floc structure initially becomes more open after flocculation. Such a trend, however, reverses in the overdosing regime. For the kaolin suspensions, the D_F value at 1000 ppm falls again. A more comprehensive data set is required, however, before attempting to rationalize such results.

A third observation is that the estimated D_S and D_F values do not correspond to each other. The fractal dimensions obtained from the light-scattering and free-settling tests are compared in Fig. 7. Apparently, for kaolin sludges, $D_F > D_S$, while for the activated sludges, $D_F < D_S$. This observation suggests that the fractal dimensions measured with different techniques provide insight into different properties of the flocs. This observation is of both academic and practical interest and is discussed further below.

DISCUSSION

As indicated above, it is apparent that the structure parameters obtained by light-scattering and free-settling velocity tests provide information on different aspects of flocculated materials. Light scattering clearly provides insight into the structure of flocculated particles at small length scales. It would seem reasonable to surmise that the structure characterized in this way is that of the "flocculi" formed by aggregation of the primary particles. While addition of polymer yields flocs that exhibit fractal behavior over a larger range of length scales than do polymer-free aggregates, we have restricted determination of the structure parameter (D_S) to a similar Q range in both polymer-free and polymer-present cases. The fact that a "loosening" of the structure of the flocculi occurs on addition of cationic polymer is suggestive of the occurrence of significant floc breakup (presumably in the rapid mix that is applied immediately after polymer addition) and a reaggregation that is now influenced by the presence of polymer attached to surface sites. The alternative scenario of flocculi penetration by polymer and subsequent reorganization would appear less likely (but not impossible). Further investigation of small-scale (flocculi) structure after polymer addition over a range of controlled mixing regimes would assist interpretation in this regard.

Flocculi presumably then attain (or approach) a steady state size that is determined by a balance between the polymer-influenced aggregating tendencies of the flocculi and disaggregation due to mixing-induced shear effects. Similar effects have recently been examined for latex flocs by Selomulya *et al.* (27, 34); investigation of the effect of controlled mixing conditions on the steady state size attained here would be particularly instructive.

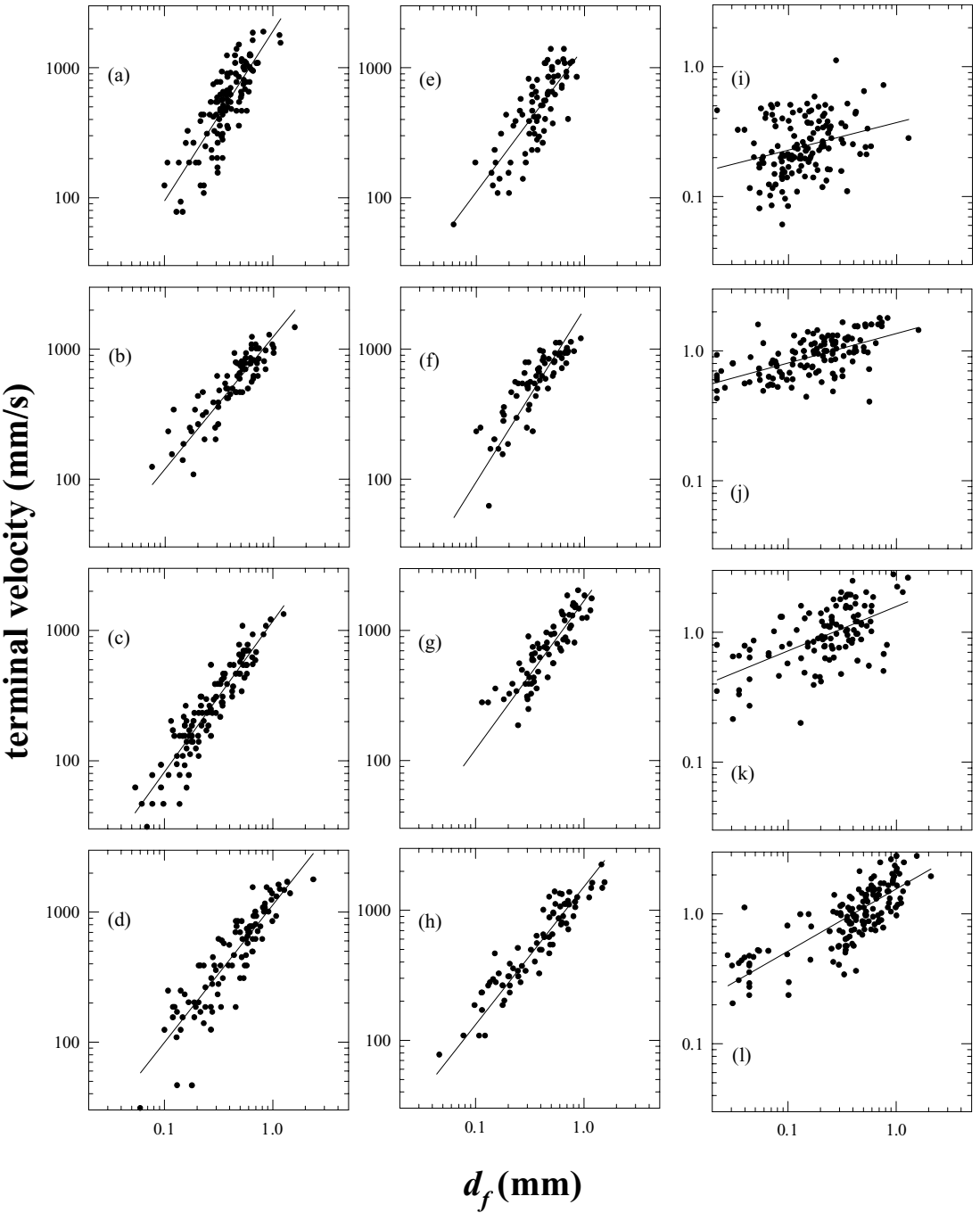

FIG. 6. Free-settling tests. (a) Kaolin sludge (8% w/w), dose = 150 ppm, slope = 1.31. (b) Kaolin sludge (8% w/w), dose = 300 ppm, slope = 0.86. (c) Kaolin sludge (8% w/w), dose = 600 ppm, slope = 1.16. (d) Kaolin sludge (8% w/w), dose = 1000 ppm, slope = 0.98. (e) Kaolin sludge (17% w/w), dose = 300 ppm, slope = 1.12. (f) Kaolin sludge (17% w/w), dose = 600 ppm, slope = 0.90. (g) Kaolin sludge (17% w/w), dose = 800 ppm, slope = 0.98. (h) Kaolin sludge (17% w/w), dose = 1000 ppm, slope = 0.94. (i) Activated sludge, original, slope = 0.55. (j) Activated sludge, dose = 10 ppm, slope = 0.31. (k) Activated sludge, dose = 30 ppm, slope = 0.34. (l) Activated sludge, dose = 40 ppm, slope = 0.48.

Reduction in mixing speed from 400 rpm (30 s) to 150 rpm (1 min) and then to 0 rpm presumably then enables the flocs to grow to the larger sizes observed. This growth process is rapid and appears to occur through polymer-induced flocculi aggregation (possibly by interflocculi bridging) rather than incremental floc growth. The structure of the "overall" flocs so produced is likely to be influenced both by the convective and gravitational forces that bring the flocculi together and (more important) the "stickiness" of the flocculi for each other, particularly as influenced by the presence of polymer. The more easily attachment

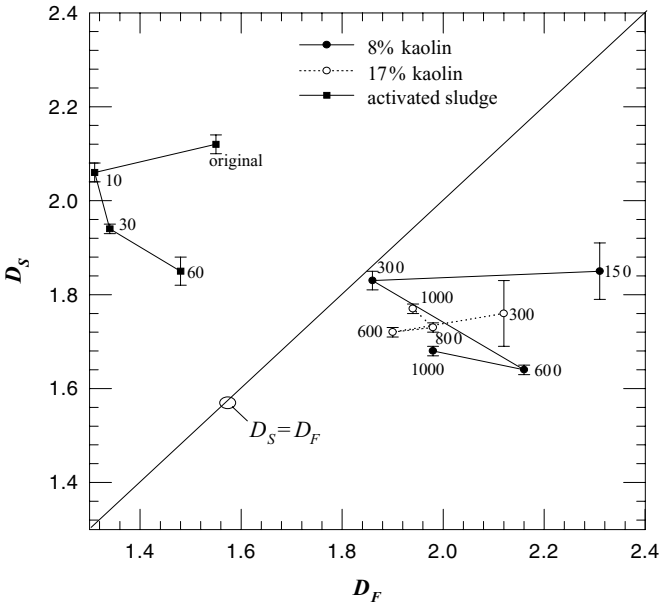

FIG. 7. D_S versus D_F plot.

occurs (and/or the more tenuous yet strong the polymer linkages), the greater the tendency to form loose overall flocs. In parallel with established determinants of floc structure in the colloidal size range (35, 36), if flocs must overcome significant barriers to interaction (typically due to charge repulsion), then they are more likely to form more compact assemblages as compared with those that attach with ease. Charge heterogeneity at flocculi surfaces may also influence the compactness of the larger flocs. Thus, if the cationic polymer adsorbs at specific sites, leaving other sites with a residual negative charge, then more compact structures may result from the resultant interaction of oppositely charged sites. (A similar phenomenon has been reported previously for iron oxide particles partially covered by natural organic matter [37].)

It will be these larger overall flocs and their size and structure characteristics that determine settling behavior. Thus, the fractal dimensions determined from the settling velocity studies reflect the impact of overall structure of these larger flocs on settling velocity. That this "overall" floc structure is different from the structure of the "building block" flocculi is perhaps not that surprising given the different conditions under which the flocculi and overall flocs were formed (i.e., rapid mix in the absence [at least initially] of polymer and slow/zero mixing conditions in the presence of polymer). It is also likely that the overall structure factors determined from settling studies may possess some spatial bias. Specifically, it is to be expected that it will be the hydrodynamic properties of the outer dimensions of the overall flocs that determines the settling behavior of flocs given that it is the extremities of flocs (rather than the smaller length scale building block flocculi) that constitute the bulk of the cross-sectional area of flocs and that are most porous. In view of this, it would appear reasonable to associate the fractal dimensions derived from settling experiments with the structure of the overall flocs generated during the period of slow (or no) mixing. The shorter length scale component of the flocs will presumably have some impact on the settling behavior, with the extent of impact depending on the size of the flocculi relative to the overall floc size. Given the limited size range of the light-scattering fractal regimes (as evident from the Q_C values), this impact would be expected to be minor in all instances considered here. We may thus ascribe the settling velocity-derived fractal dimension to the structure of the flocs formed under low (or no) mixing.

It is interesting that the larger length scale structure of the activated sludge flocs is significantly lower than that of the core. This result may reflect the occurrence of restructuring of the inner portion due to rapid mixing but more likely reflects the "stickiness" of activated sludge flocs when dosed with cationic polymer with resultant formation of very loose assemblages made up of aggregated flocculi. In comparison, the larger length scale structure of the clay assemblages appears to be somewhat more compact than the core. As indicated above, such a result could arise from greater charge repulsion; however, the zeta potential results (Figs. 2a and 2b) do not bear this out. Alternatively, the cationic polymer may bind at specific kaolinite surface sites, leaving the kaolinite particles the opportunity for strong coupling due to attractive electrostatic effects. Such conclusions are somewhat speculative, however, and additional work is required to explain the magnitude of these structure parameters of these apparently "multifractal" assemblages.

In summary, then, we conclude that the assemblages of kaolin and activated sludge examined here possess multiple levels of structure, with both the size and structure characteristics determined to a large extent by the mixing conditions under which these flocs were formed and the subsequent effects of polymer in inducing rapid aggregation of flocculi. Light scattering appears to be a useful method of probing the structure of smaller flocculi formed when primary particles interact and attain some steady state size and structure under conditions of rapid mixing, although further attention should be given to possible effects on structure determination of multiple scattering within the more compact flocs (32, 33). In comparison, structural information derived from settling velocity investigations appears to provide insight into the structure of the overall flocs, but with a bias toward the properties of the outer portions of flocs formed under minimal (or no) mixing.

CONCLUSIONS

Aggregates occurring naturally can be viewed as fractals of fractals, which need two or more fractal dimensions as structural descriptors. This work compared the estimated fractal dimensions from a light-scattering test (D_S) and a free-settling test (D_F), using two kaolin suspensions and a waste activated sludge as the testing materials. Discrepancies in the estimated D_S and D_F values indicated that the fractal dimension is an operationally

defined value. The addition of polyelectrolyte monotonically decreased D_S, and the D_F versus polymer dose curve exhibited a minimum at the optimum dose. For kaolin sludge, $D_F > D_S$, and for activated sludge, $D_F < D_S$. Meanwhile, the sizes of both the entire floc and the scattered aggregates increased with polymer dose, with the former larger than the latter.

A two-level floc structural model, which represents the formation of a primary floc (of dimension D_S) from primary particles and of an entire floc (of dimension D_F) from microflocs, is proposed to interpret the experimental findings. After flocculation, the compactness of both the primary flocs and the entire flocs changed markedly. The compactness of the interior structure of the primary flocs exhibited no correlation with the occurrence of charge neutralization or with sludge dewaterability. However, the global structure of the entire flocs in the kaolin sludge was controlled by the surface charge, closely corresponding to the occurrence of the minimum CST values.

REFERENCES

1. Li, D. H., and Ganczarczyk, J., *Envir. Sci. Tech.* **23,** 1385 (1989).
2. Jiang, Q., and Logan, B. E., *Envir. Sci. Tech.* **25,** 2031 (1991).
3. Li, D. H., and Ganczarczyk, J., *Biotechnol. Bioeng.* **35,** 57 (1990).
4. Zartarian, F., Mustin, C., Villemin, G., Ait-Ettager, T., Thill, A., Bottero, J. Y., Mallet, J. L., and Snidaro, D., *Langmuir* **13,** 35 (1997).
5. Tambo, N., and Watanabe, Y., *Water Res.* **13,** 409 (1979).
6. Mitani, T., Unno, H., and Akekata, T., *Jpn. Water Res.* **6,** 65 (1983).
7. Li, D. H., and Ganczarczyk, J., *Water Res.* **21,** 257 (1987).
8. Li, D. H., and Ganczarczyk, J., *Water Envir. Res.* **64,** 236 (1992).
9. Huang, H., *Clays Clay Miner.* **41,** 373 (1993).
10. Lee, D. J., and Hsu, Y. H., *Envir. Sci. Tech.* **28,** 1444 (1994).
11. Lee, D. J., Chen, G. W., Liao, Y. C., and Hsieh, C. C., *Water Res.* **30,** 541 (1996).
12. Axford, D. T., and Herrington, T. M., *J. Chem. Soc. Faraday Trans*. **90,** 2085 (1994).
13. Zhang, J., and Buffle, J., *Colloid Surfaces A* **107,** 175 (1996).
14. Kyriakidis, A. S., Yiantsios, S. G., and Karabelas, A. J., *J. Colloid Interface Sci.* **195,** 299 (1997).
15. Jung, S. J., Amal, R., and Rpper, J. A., *Part. Part. Syst. Charact*. **12,** 274 (1995).
16. Guan, J., Waite, T. D., Wukasch, R., and Amal, R., "Rapid Determination of Fractal Structure of Bacterial Assemblages in Wastewater Treatment: Implications to Process Optimisation, pp. 200–207. IAWQ Biennial International Conference, Vancouver, British Colombia, June 1998.
17. Guan, J., Waite, T. D., and Amal, R., *Envir. Sci. Tech.* **32,** 3735 (1998).
18. Guan, J., "Implications of Floc Structure to Solid–Liquid Separation Processes in Wastewater Treatment." Ph.D. thesis, University of New South Wales, Australia, 1999.
19. Clark, M. M., and Flora, J. R. V., *J. Colloid Interface Sci.* **147,** 407 (1991).
20. Jorand, F., Zartarian, F., Thomas, F., Block, J. C., Bottero, J. Y., Villemin, G., Urbain, V., and Manem, J., *Water Res*. **29,** 1639 (1995).
21. Sanin, F. D., and Vesilind, P. A., *Water Envir. Res*. **68,** 927 (1996).
22. Gorczyca, B., and Ganczarczyk, J., *Water Qual. Res. J. Can.* **34,** 653 (1999).
23. Lee, D. J., *Water Res.* **33,** 1116 (1999).
24. Lin, M. Y., Lindsay, H. M., Weitz, D. A., Ball, R. C., Klein, R., and Meakin, P., *Nature* **339,** 360 (1989).
25. Bushell, G., and Amal, R., *J. Colloid Interface Sci*. **221,** 186 (2000).
26. Van de Hulst, H. C., "Light Scattering by Small Particles," Dover, New York, 1981.
27. Selomulya, C., Amal, R., Bushell, G., and Waite, T. D., *J. Colloid Interface Sci*. **236,** 66 (2001).
28. Farias, T. L., Köylü, Ü. Ö., and Carvalho, M. G., *Appl. Optics* **35,** 6560 (1996).
29. Bushell, G., Yan, Y. D., Woodfield, D., Raper, J., and Amal, R., *Adv. Colloid Interface Sci*. **95,** 1 (2002).
30. Wu, R. M., and Lee, D. J., *Water Res.* **32,** 860 (1998).
31. Wu, R. M., and Lee, D. J., *Chem. Eng. Sci.* **54,** 5717 (1999).
32. Lambert, S., Thill, A., Ginestet, P., Audic, J. M., and Bottero, J. Y., *J. Colloid Interface Sci.* **228,** 379 (2001).
33. Thill, A., Lambert, S., Moustier, S., Ginestet, P., Audic, J. M., and Bottero, J. Y., *J. Colloid Interface Sci.* **228,** 386 (2001).
34. Selomulya, C., Amal, R., Bushell, G., and Waite, T. D., *Langmuir* **18,** 1974 (2002).
35. Lin, M. Y., Klein, R., Lindsay, H. M., Weitz, D. A., Ball, R. C., and Meakin, P., *J. Colloid Interface Sci.* **137,** 263 (1990).
36. Waite, T. D., *Colloids Surfaces* **151,** 27 (1999).
37. Amal, R., Raper, J. A., and Waite, T. D., *J. Colloid Interface Sci*. **151,** 244 (1992).